



UNIVERSITY OF LEEDS

This is a repository copy of *Tissue-Specific RNAi Tools to Identify Components for Systemic Stress Signaling*.

White Rose Research Online URL for this paper:
<http://eprints.whiterose.ac.uk/161827/>

Version: Accepted Version

Article:

Miles, J orcid.org/0000-0001-8839-9201 and van Oosten-Hawle, P orcid.org/0000-0002-5713-6457 (2020) *Tissue-Specific RNAi Tools to Identify Components for Systemic Stress Signaling*. *Journal of Visualized Experiments*, 159. e61357. ISSN 1940-087X

<https://doi.org/10.3791/61357>

© 2020 Journal of Visualized Experiments. This is an author produced version of an article published in *Journal of Visualized Experiments*. Uploaded in accordance with the publisher's self-archiving policy.

Reuse

Items deposited in White Rose Research Online are protected by copyright, with all rights reserved unless indicated otherwise. They may be downloaded and/or printed for private study, or other acts as permitted by national copyright laws. The publisher or other rights holders may allow further reproduction and re-use of the full text version. This is indicated by the licence information on the White Rose Research Online record for the item.

Takedown

If you consider content in White Rose Research Online to be in breach of UK law, please notify us by emailing eprints@whiterose.ac.uk including the URL of the record and the reason for the withdrawal request.



eprints@whiterose.ac.uk
<https://eprints.whiterose.ac.uk/>

1 **TITLE:**

2 **Tissue-Specific RNAi Tools to Identify Components for Systemic Stress Signaling**

3
4 **AUTHORS & AFFILIATIONS:**

5 Jay Miles, Patricija van Oosten-Hawle

6
7 School of Molecular and Cell Biology & Astbury Centre for Structural Molecular Biology,
8 University of Leeds, Leeds, United Kingdom

9
10 bsjmi@leeds.ac.uk

11
12 Corresponding Author:

13 Patricija van Oosten-Hawle

14 p.vanoosten-hawle@leeds.ac.uk

15
16 **KEYWORDS:**

17 proteostasis, tissue-specific, chaperone reporters, *C. elegans*, cell-nonautonomous, stress
18 response, Transcellular chaperone signaling

19
20 **SUMMARY:**

21 Maintenance of organismal proteostasis requires the coordination of protein quality control
22 responses such as chaperone expression from one tissue to another. Here, we provide tools used
23 in *C. elegans* that allow monitoring of proteostasis capacity in specific tissues and determine
24 intercellular signaling responses.

25
26 **ABSTRACT:**

27 Over the past decade, regulation of protein quality control processes went through a
28 transformation that unveiled the importance of intercellular signaling processes to regulate cell-
29 nonautonomous proteostasis. Recent studies are now beginning to uncover signaling
30 components and pathways that coordinate protein quality control from one tissue to another. It
31 is therefore important to identify mechanisms and components of the cell-nonautonomous
32 proteostasis network (PN) and its relevance for aging, stress responses and protein misfolding
33 diseases. In the laboratory, we use genetic knockdown by tissue-specific RNAi in combination
34 with stress reporters and tissue-specific proteostasis sensors. We describe methodologies to
35 examine and to identify components of the cell-nonautonomous PN that can act in tissues
36 perceiving a stress condition and in responding cells to activate a protective response. We first
37 describe how to generate hairpin RNAi constructs for constitutive genetic knockdown in specific
38 tissues and how to perform tissue-specific genetic knockdown by feeding RNAi at different life
39 stages. Stress reporters, and behavioral assays then function as a valuable readout, that allow for
40 the fast screening of genes and conditions modifying systemic stress signaling processes. Finally,
41 proteostasis sensors expressed in different tissues are utilized to determine changes in the tissue-
42 specific capacity of the PN at different stages of development and aging. Thus, these tools should
43 help clarify and allow monitoring the capacity of PN in specific tissues, while helping to identify
44 components that function in different tissues to mediate cell-nonautonomous PN in an organism.

45

46 **INTRODUCTION:**

47 Cellular proteostasis is monitored by an intricate network of protein quality control components
48 such as molecular chaperones, stress responses and degradation mechanisms including the
49 ubiquitin proteasome system (UPS) and autophagy^{1,2}. The activation of stress response
50 pathways, such as the HSF-1 mediated heat shock response (HSR), the unfolded protein response
51 of the endoplasmic reticulum (UPR^{ER}) and the mitochondria (UPR^{mito}) is vital for cellular
52 adaptation to and survival during environmental challenges or protein misfolding disease that
53 lead to toxic protein aggregation¹⁻⁶.

54

55 Cellular proteostasis is coordinated by an additional layer in multicellular organisms that requires
56 the orchestration of cellular stress responses across different tissues to activate protective
57 protein quality control components such as molecular chaperones⁷. In the past decade, cell
58 nonautonomous activation of “cellular” stress response pathways has been observed for the heat
59 shock response (HSR), the UPR^{ER} and the UPR^{mito}, as well as transcellular chaperone signaling
60 (TCS)^{3,4,7-10}. In each case, the nervous system as well as signaling from the intestine plays a crucial
61 role in controlling the activation of chaperones across tissues, to protect against the toxic
62 consequences of acute and chronic protein misfolding stresses^{3,5,9,11}. This transmission from the
63 neurons to the intestine and other cells in the periphery can be achieved by neurotransmitters
64 as is the case for the UPR^{ER} and the HSR^{6,8,11}. In one form of cell nonautonomous stress signaling,
65 TCS, that is activated by the increased expression of HSP-90 in the neurons, secreted immune
66 peptides play a role in the activation of *hsp-90* chaperone expression from the neurons to the
67 muscle⁵. In another form of TCS, reducing the expression of the major molecular chaperone *hsp-*
68 *90* in the intestine leads to an increased expression of heat-inducible *hsp-70* at permissive
69 temperature in the body wall muscle^{5,10}. In this particular case, the specific signaling molecules
70 activated in the stress-perceiving intestine and the responding muscle cells are, however,
71 unknown.

72

73 Thus, in order to identify how chaperone expression is activated from one tissue to another, an
74 approach is required that allows to monitor the capacity of the proteostasis network (PN) and
75 stress response activation at the tissue-specific level. To investigate which stress response
76 pathway is activated in the individual tissues, an available selection of transcriptional chaperone
77 reporters fused to fluorescent protein tags can be utilized (see also **Table 3**). These include
78 fluorescently tagged *hsp-90*, *hsp-70* and *hsp-16.2* transcriptional reporters that indicate the
79 induction of the HSR, *hsp-4* that indicates the activation of the UPR^{ER} and *hsp-6*, indicating the
80 UPR^{mito}. Combination of these reporters with a tissue-specific stress condition then allows a
81 powerful read-out that will pin-point individual tissues responding to an imbalance of the PN in
82 a distal “sender” tissue perceiving the stress. To induce a stress condition or imbalance of the PN
83 in a specific tissue, different approaches can be taken. For example, one such approach is by
84 ectopic expression of the activated form of a stress transcription factor (e.g., *xbp-1s*) and another
85 one is by reducing the expressing levels of an essential molecular chaperone (e.g., *hsp-90*) using
86 tissue-specific promoters^{8,10}. To deplete PN components in only one cell type, tissue-specific
87 knockdown by RNAi is a useful tool.

88

89 In *C. elegans*, RNAi is however systemic; double stranded RNA in the environment can enter and
90 spread throughout the animal to silence a targeted gene^{12,13}. This systemic spread of ingested
91 dsRNA is mediated by SID (systemic RNAi defective) proteins, such as SID-1 and SID-2 proteins
92 that are dsRNA transporters, as well as SID-5, that colocalizes with late endosome proteins and
93 is implicated in the export of ingested dsRNA¹⁴⁻¹⁶. SID-1 is a multi-pass transmembrane protein
94 in all cells (except neurons) and required for dsRNA export as well as import into cells¹⁷. SID-2
95 expression is restricted to the intestine where it functions as an endocytic receptor for ingested
96 dsRNA from the intestinal lumen into the cytoplasm of intestinal cells¹⁶. Neurons lack a response
97 to systemic RNAi, and this correlates with reduced expression of the transmembrane protein SID-
98 1 in neurons, that is essential for dsRNA to be imported^{15,18}. Thus, for tissue-specific RNAi to be
99 effective in only one cell-type, the systemic spread of dsRNA needs to be prevented. This can be
100 achieved by utilizing the RNAi-resistant *sid-1(pk3321)* mutant that prevents the release and
101 uptake of dsRNA across tissues¹⁵. Expression of a tissue-specific hairpin RNAi construct in this
102 mutant or the ectopic expression of SID-1 in a specific tissue can then complement the function
103 of mutant *sid-1* and will allow for tissue-specific RNAi¹⁹.

104
105 So how is dsRNA ingested by the intestine in a *sid-1* loss of function mutant and how can it then
106 reach neurons or muscle cells that ectopically express a SID-1 construct? In one current model
107 explaining this mechanism, endocytosed dsRNA is taken up into the intestinal cytoplasm via SID-
108 2 and then exported into the pseudocoelom by another SID-1 independent mechanism, involving
109 SID-5 and transcytosis¹⁷. Thus because SID-1 is required for dsRNA import¹⁷, only cells expressing
110 wild type SID-1 will be able to take up the dsRNA released from the intestine into the
111 pseudocoelom.

112
113 Here we demonstrate the use of a set of tools that allow for tissue-specific RNAi. We use the
114 example of the molecular chaperone Hsp90 to describe the construction of hairpin RNAi that can
115 be useful to constitutively knock down gene expression in a specific tissue¹⁰. The described
116 approach could be used for any target gene of interest. The response of other tissues to the
117 proteostasis imbalance caused by tissue-specific *hsp-90* RNAi can be probed by monitoring the
118 expression of fluorescently tagged stress reporters in other tissues. As a second method for
119 tissue-specific RNAi, we demonstrate how the *sid-1* mutant system can be adapted for feeding
120 RNAi bacteria rather than expression of a hairpin RNAi construct. This can be useful when
121 performing a candidate or genome-wide RNAi screen to identify components required for a
122 tissue-specific response. Likewise, developmental defects associated with depletion of a vital PN
123 component will require RNAi-mediated knockdown in specific tissues at later stages of
124 development. We demonstrate how a SID-1 complementation system can be used on a candidate
125 RNAi screen for tissue-specific TCS modifiers. In the example, we aim to identify signaling
126 components that upon knockdown in the “stress-perceiving” sender tissue (intestine) and the
127 stress effecting tissue (muscle) lead to the changed expression of a fluorescently tagged *hsp-70*
128 reporter in muscle cells.

129
130 **PROTOCOL:**
131

132 **1. Tissue-specific RNAi in two ways: Hairpin RNAi and tissue-specific SID-1**

133 **complementation**

134

135 1.1. Generation of hairpin RNAi constructs for tissue-specific expression in *sid-1* mutants

136

137 1.1.1. Amplify the target gene sequence (e.g., *hsp-90* sequence isolated from the *hsp-90* RNAi
138 clone from the Ahringer RNAi library²⁰) by PCR. Place a nonpalindromic sequence at the 3' end of
139 the *hsp-90* sequence, that is a Sfil site (ATCTA)²¹.

140

141 NOTE: The primers used for cloning the *hsp-90* with the Sfil sequence (underlined) are:

142 *as-hsp90-Sfil* 5'-GGCCATCTAGGCCCTGGGTTGATTTTCGAGATGCT-3'

143 *as-hsp90* 5' TCATGGAGAACTGCGAAGAGC-3'.

144

145 1.1.2. Subclone the amplified sequence into the commercial cloning kit (e.g., TOPO pCR BluntII).

146

147 1.1.3. Isolate the inverted *hsp-90* sequence from the *hsp-90* RNAi clone (Ahringer RNAi library)²⁰
148 by restriction digestion using XbaI and PstI restriction sites and place it downstream of the *hsp-*
149 *90-Sfil* sequence in the vector (from step 1.1.1), resulting in an *hsp-90* hairpin construct (**Figure**
150 **1**).

151

152 1.1.4. Subclone the hairpin construct into a Gateway entry vector pDONR221 and fused with
153 Gateway entry clones that contain tissue-specific promoters for either expression in neurons
154 (*rgef-1p*); in the intestine (*vha-6p*); or the bodywall muscle (*unc-54p*) and the *unc-54* 3'UTR (or
155 any other 3'UTR of choice) in a Gateway reaction as described in the protocol of the supplier.

156

157 1.1.5. Linearize the resulting hairpin RNAi constructs (**Figure 1**) using a unique restriction site
158 outside the coding sequence and microinject as a complex array at a concentration of 1 ng/μL
159 hairpin RNAi construct, mixed with 100 ng/μL N2 Bristol genomic DNA (digested with Scal) into a
160 *C. elegans* strain expressing the *hsp-70p::RFP* reporter (strain AM722) and crossed into the
161 genetic background of *sid-1(pk3321)* mutants (strain NL3321). For a protocol on how to perform
162 microinjection of complex arrays please follow²².

163

164 1.1.6. As a negative control, use empty vector hairpin constructs expressing the nonpalindromic
165 Sfil containing sequence (GGCCATCTAGGCC) under control of a tissue-specific promoter.

166

167 1.1.7. Use the increased *hsp-70p::RFP* expression of the reporter as a readout to score positive
168 transformants expressing *hsp-90* hairpin RNAi (**Figure 3**). For a more general approach to verify
169 the tissue-specific knock-down of any gene of interest, measure whole animal mRNA levels using
170 qRT-PCR of the gene of interest.

171

172 1.1.8. Integrate the extrachromosomal array of the resulting strain expressing the intestine-
173 specific *hsp-90* hairpin construct (PVH2; see Table 1) by gamma-irradiation. For integration of the
174 extrachromosomal arrays into the genome, please see²².

175

176 1.2. Tissue-specific SID-1 expression to allow for tissue-specific RNAi by feeding dsRNA-

177 expressing bacteria

178

179 1.2.1. Subclone the *sid-1* genomic DNA from vector TU867 (*unc-119p::SID-1*)¹⁹ into the Gateway
180 entry vector pDONR221. Primers for cloning of *sid-1* DNA can be found in¹⁹. Fuse the *sid-1*
181 pDONR221 construct with Gateway entry clones containing muscle- (*myo-3p*) or intestine- (*vha-*
182 *6p*) specific promoters and the *unc-54 3'UTR* (or any other 3'UTR of choice) in the Gateway
183 reaction as described before in 1.1.4.

184

185 1.2.2. Microinject the resulting *vha-6p::SID-1::unc-54 3'UTR* or *myo-3p::SID-1::unc-54 3'UTR*
186 constructs at a concentration of 30 ng/μL together with a red fluorescent pharyngeal co-injection
187 marker (e.g., *myo-2p::RFP*; 5 ng/μL) into *sid-1(pk3321)* mutants.

188

189 1.2.3. Integrate the extrachromosomal intestine- or muscle-specific *sid-1* arrays into the
190 genome as described in²². Here, this resulted in strains PVH5 [*myo-3p::SID-1*; *myo-2p::RFP*];*sid-*
191 *1(pk3321)* and PVH65 [*vha-6p::SID-1*; *myo-2p::RFP*];*sid-1(pk3321)*.

192

193 1.2.4. For neuron-specific expression of *sid-1* in the *sid-1(pk3321)* mutant, use strain TU3401
194 *uls3401[unc-119p::SID-1*; *myo-2p::RFP*];*sid-1(pk3321)* that was generated previously by Calixto
195 et al.¹⁹.

196

197 1.2.5. As mentioned in 1.1.7, ensure tissue-specific knockdown of the gene of interest by
198 measuring mRNA levels of the desired target gene by qRT-PCR. Alternatively, confirm tissue-
199 specific RNAi sensitivity by using a fluorescent protein (e.g., GFP or RFP) expressed in the same
200 tissue and treat worms with GFP or RFP RNAi. Expose nematodes to GFP/RFP RNAi as
201 synchronized L1 stage larvae and grow on the RNAi bacteria until Day 1 of adulthood (see **Figure**
202 **2**). In our case, we used strains expressing SID-1 in the neurons, muscle or intestine and crossed
203 into strains expressing HSP-90::RFP in neurons (AM987), in the intestine (AM986) and in the
204 muscle (AM988).

205

206 **2. Using stress reporters and proteostasis sensors to monitor cell autonomous and cell** 207 **nonautonomous proteostasis**

208

209 NOTE: To monitor PN capacity in specific tissues, use tissue-specific proteostasis sensors (such as
210 strains expressing Q44 in the intestine or Q35 in the muscle – see **Table 3**) and stress reporters
211 (such as the heat-inducible *hsp-70p::mCherry* reporter; **Table 3**).

212

213 2.1. Genetically crossing the *sid-1 (pk3321)* mutant allele into a proteostasis sensor strain and
214 confirming the presence of *sid-1(pk3321)* by feeding RNAi

215

216 2.1.1. Genetically cross the proteostasis sensor/stress reporter strain into the genetic
217 background of the *sid-1 (pk3321)* mutant strain. To establish genetic crosses between different
218 transgenic strains, please follow²³ for a detailed protocol.

219

220 NOTE: *sid-1(pk3321)* mutants are resistant to feeding RNAi and hence treatment of embryos with

221 RNAi against an essential gene (such as *elt-2* or *hsp-90*) will only lead to developmental arrests
222 or larval lethality in strains heterozygous or wildtype for the *sid-1* gene.

223

224 2.1.2. Let 10 gravid hermaphrodites lay eggs on RNAi plates against *elt-2* or *hsp-90* and control
225 (empty vector; EV) RNAi plates at 20 °C. Remove the mothers after 1 - 2 h. Use N2 Bristol and the
226 *sid-1(pk3321)* mutant as controls.

227

228 2.1.3. Observe development of the larvae on the RNAi plates over the next 2-3 days. *elt-2* RNAi
229 will result in L1 larval arrest, while *hsp-90* RNAi results in L3 larval arrest in N2 Bristol. *sid-1*
230 mutants will be unaffected by the RNAi treatment and will develop into gravid adults.

231

232 NOTE: *C. elegans* homozygote for *sid-1(pk3321)* will show a uniform population developing into
233 adulthood. Heterozygotes will be indicated by mixed populations of some animals showing larval
234 arrest, and some animals developing into adults.

235

236 2.2. Confirming the presence of *sid-1(pk3321)* by genotyping

237

238 2.2.1. Pick 15-20 worms of the selected candidate F2 strain into a PCR tube containing 15 µL of
239 Worm Lysis Buffer (**Table 2**).

240

241 2.2.2. Place the tube at -80 °C for at least 10 min or overnight.

242

243 2.2.3. Incubate the tube in the PCR machine using the following program:
244 65 °C for 60 min (lyse worm); 95 °C for 15 min (inactivate Proteinase K); hold at 4 °C.

245

246 2.2.4. Use 2 µL of the worm lysate as a “template” to perform the PCR reaction for genotyping,
247 using the following primers for *sid-1*: *sid-1 forw*: 5'-agctctgtacttgattcg-3' and *sid-1 rev*: 5'-
248 gcacagttatcagatttg-3'.

249

250 2.2.5. Use the following program for PCR genotyping: 1 cycle at 95 °C for 3 min; then 30 cycles
251 of 95 °C for 10 s, 55 °C for 30 s, and 72 °C for 30 s; 1 cycle at 72 °C for 10 min, hold at 4 °C.

252

253 2.2.6. Purify the ~650 bp PCR product using a PCR purification kit (**Table of Materials**) and
254 sequence the *sid-1* PCR product to identify the G-to-A point mutation of the *sid-1 (pk3321)* allele.
255 Alternatively, the G-to-A point mutation creates an Apol restriction site, which can be used on
256 the PCR product for genotyping as described in ²⁴.

257

258 **2.3. Using *iQ44::YFP* as a proteostasis sensor for the intestine**

259

260 2.3.1. Synchronize *C. elegans* expressing Q44::YFP in the intestine (strain OG412) or crossed into
261 the *sid-1(pk3321)* mutant background by bleaching, following the protocol described in ²⁵. Plate
262 synchronized L1 larvae onto a 9 cm nematode growth media (NGM)-agar plate containing OP50
263 bacteria and grow until L4 stage at 20 °C.

264
265 2.3.2. Collect L4 animals by washing worms off the plate using 5 mL of M9 buffer. Transfer the
266 M9 buffer containing L4 worms to a 15 mL tube using a glass pipette or a siliconized plastic
267 pipette, and centrifuge at 1000 x *g* for 1 min at room temperature to gently pellet the worms.
268 Remove the supernatant carefully, ensuring to leave the worm pellet undisturbed.

269
270 2.3.3. Critical Step: To transfer or plate out nematodes use a glass pipette or a plastic pipette
271 tip that was treated with a siliconizing agent (e.g., SigmaCote) following the manufacturer's
272 instruction. This prevents the sticking of worms to the plastic surface of a pipette tip.

273
274 2.3.4. Repeat step 2.3.2 three more times to wash off all OP50 bacteria from the worms.

275
276 2.3.5. Take up the worm pellet in 5 mL of M9 buffer and count the number of worms present in
277 10 μ L.

278
279 2.3.6. Plate L4 animals on 6 cm NGM Agar plates containing empty vector control (EV) or *hsp-*
280 *90* RNAi bacteria at a density of 10 worms per plate (prepare 5 plates per time point and biological
281 replicate) and incubate for 24 -48 hours at 20 °C.

282
283 2.3.7. After 24 hours (=Day 1 adults) and 48 hours (=Day 2 adults) count the number of Q44 foci
284 in the intestines of nematodes exhibiting aggregates. Score a total of at 30-50 nematodes per
285 biological replicate.

286 287 **3. Tissue-specific candidate RNAi screen for modifiers of cell nonautonomous proteostasis**

288
289 NOTE: For the tissue-specific RNAi screen we used strain PVH172 allowing for intestine-specific
290 RNAi by feeding RNAi bacteria and strain PVH171 allowing for muscle-specific RNAi (see Table 1
291 for genotype).

292 293 **3.1. Preparation of the candidate RNAi plates**

294
295 3.1.1. Prepare 6 cm NGM agar plates supplemented with 100 μ g/mL ampicillin, 12.5 μ g/mL
296 tetracycline and 1 mM IPTG according to standard methods²⁵.

297
298 3.1.2. Use the Ahringer RNAi library to obtain the candidate RNAi clones for the RNAi screen²⁰.

299
300 3.1.3. Inoculate 3 mL of LB-amp media (50 μ g/mL ampicillin in LB media) in at 15 mL tube with
301 the desired RNAi clone using a plastic pipette tip. Grow at 37 °C overnight with agitation.

302
303 3.1.4. The next day add Isopropyl-b-D-thiogalactopyranosid (IPTG) (from a 1 M stock) to a final
304 concentration of 1 mM in the bacterial overnight culture.

305
306 3.1.5. Agitate the cultures for a further 3 h at 37 °C.

307

308 3.1.6. Plate 300 μ L of bacterial RNAi culture onto a 6 cm NGM agar plate supplemented with 100
309 μ g/mL ampicillin, 12.5 μ g/mL tetracycline and 1 mM IPTG. Let the plates dry on the bench for 2
310 days at room temperature, covered with aluminum foil to protect from light. Once dry, the RNAi
311 plates can be stored in a box at 4 $^{\circ}$ C for several weeks.

312

313 3.2. Synchronization of *C. elegans* and treatment with RNAi bacteria

314

315 3.2.1. To synchronize worm strains, pick 15 gravid adults onto RNAi plates and allow to lay eggs
316 for 1 h. Then remove the adults from the plate.

317

318 **Critical step:** Synchronization by bleaching is avoided in this case, because it can induce the *hsp-*
319 *70p::RFP* reporter, as it is a stressful condition for *C. elegans*.

320

321 3.2.2. Pick synchronized L4 stage larvae and transfer to a fresh RNAi plate.

322

323 3.2.3. Allow nematodes to grow on the relevant RNAi for two generations to ensure efficient
324 uptake of dsRNA, making sure the temperature is kept at 20 $^{\circ}$ C.

325

326 3.2.4. For imaging and *hsp-70p::RFP* fluorescence quantification, use Day 1 adults.

327

328 3.3. Preparation of microscope slides

329

330 3.3.1. Prepare the microscope slides by placing \sim 250 μ L of a 2% agarose solution (in M9 buffer)
331 onto a glass microscope slide and a second slide place on top to create a flat disc.

332

333 3.3.2. Place 5 μ L of 5 mM Levamisole solution (in M9 buffer) on the set agarose pad and transfer
334 5 Day 1 adult worms into the Levamisole drop. Leave the nematodes to paralyze for 5 min.

335

336 3.3.3. Once *C. elegans* are paralyzed, carefully align with a platinum wire pick and remove excess
337 levamisole with a laboratory wipe before addition of a coverslip.

338

339 3.3.4. **Critical step:** Ensure to take images of the worms within 30 minutes after preparation of
340 the microscope slides. Paralyzed nematodes on the microscope slide can dry out and burst, which
341 can compromise the fluorescence measurements.

342

343 3.4. Microscope settings and image analysis

344

345 **NOTE:** Images are obtained using a confocal microscope equipped with an EM-CCD camera and
346 a microscopy image automation & image analysis software.

347

348 3.4.1. Take images at 10x magnifications using a 561 nm laser for RFP fluorescence excitation.
349 Ensure all images are taken using the same settings for laser power, pinhole size and fluorescence
350 gain to enable comparisons.

351

352 3.4.2. Save all images as TIFF files.

353

354 3.4.3. Perform image analysis using ImageJ. Measure fluorescence intensity in each image as
355 pixels per unit area, with background fluorescence subtracted. Normalize fluorescence intensity
356 for each image to the image area as well as the length of the worms.

357

358 3.4.4. Measure the mean intensity using **Analyze | Measure** in ImageJ. Normalize the resulting
359 intensity value to the image area by dividing the intensity by area.

360

361 3.4.5. To normalize the intensity to worm length, measure the worm by drawing a line along the
362 length of the worm in ImageJ and using **Analyze | Measure**. The reason for normalizing
363 fluorescence intensity to worm length, is that worms can vary in size, dependent on the gene
364 that is knocked down by RNAi, and this could affect the mean intensity.

365

366 3.4.6. Normalize the measured fluorescence intensities to untreated controls (i.e., transgenic *C.*
367 *elegans* grown on control (EV) RNAi plates). Pool the normalized values to compare mean
368 fluorescence intensities for each RNAi condition. Aim to image 20 worms per biological replicate
369 and collect at least 3 biological replicate images.

370

371 3.4.7. Calculate P-values of the mean fluorescence intensity values using student's t test and
372 perform a correction for multiple testing using the Benjamini-Hochberg method, using a false
373 discovery rate of 0.01.

374

375 **REPRESENTATIVE RESULTS:**

376 **Tissue-specific RNAi in two ways: Expression of hairpin constructs or tissue-specific SID-1** 377 **complementation**

378 Expression of tissue-specific hairpin RNAi constructs allows for constitutive knockdown of a gene
379 throughout development. However this can sometimes be impractical when the surveyed gene
380 is required for organogenesis of that particular tissue, such as *elt-2* which is required for
381 development of the intestine²⁶. Tissue-specific SID-1 expression in the RNAi-resistant *sid-1*
382 mutants has the particular advantage that tissue-specific gene knockdown can be timed at later
383 stages of development. In both cases (for the expression of a hairpin construct or tissue-specific
384 SID-1 complementation), the efficiency of the tissue-specific RNAi needs to be validated to
385 confirm that only the targeted tissue is affected by RNAi. This is accomplished by co-expressing a
386 fluorescently tagged protein such as HSP-90 fused to RFP (HSP-90::RFP) in different tissues.

387

388 We genetically crossed *sid-1(pk3321)* mutants alone or *sid-1* mutants expressing SID-1 in either
389 neurons, intestine or bodywall muscle into *C. elegans* expressing HSP-90::RFP in the neurons
390 (**Figure 2A**), intestine (**Figure 2B**) or the muscle (**Figure 2C**). The resulting strains were treated
391 with *hsp-90* RNAi at L4 stage for 24 hours and HSP-90::RFP expression in specific tissues was
392 examined by fluorescence microscopy.

393

394 *HSP-90::RFP^{neuro}* animals expressing SID-1 in the neurons (*unc-119p::SID-1*) exhibit reduced
395 expression of HSP-90::RFP in neurons of the magnified tail region (**Figure 2A**). Likewise, *HSP-*

396 *90::RFP^{int}* animals expressing SID-1 in the intestine (*vha-6p::SID-1*) show reduced HSP-90::RFP
397 expression in the intestine as expected (**Figure 2B**), whereas *sid-1(pk3321)* mutants expressing
398 HSP-90::RFP in the intestine are unaffected by feeding *hsp-90* RNAi. Intestinal HSP-90::RFP
399 expression also remains unaffected in animals expressing SID-1 in the neurons or the bodywall
400 muscle, indicating that dsRNA is not spreading from the muscle or the neurons to the intestine
401 (**Figure 2B**). Conversely, *HSP-90::RFP^{muscle}* animals expressing SID-1 in the muscle (*myo-3p::SID-1*)
402 exhibit reduced HSP-90::RFP expression in the muscle during *hsp-90* RNAi, while HSP-90::RFP
403 levels are unaffected in worms expressing SID-1 in the neurons or intestine (**Figure 2C**).
404

405 **Using a stress reporter for a tissue-specific candidate RNAi screen**

406 Reducing the function or expression of the major molecular chaperone HSP-90 induces the heat
407 shock response and HSP-70 chaperone expression²⁷. Tissue-specific *hsp-90* RNAi in the *C. elegans*
408 intestine results in a strong upregulation of *hsp-70* in the muscle, as well as other tissues, as
409 indicated by the stress-inducible *hsp-70* reporter (*hsp-70p::RFP*) (**Figure 3A**)¹⁰. *hsp-70* is a heat-
410 inducible chaperone, and thus no expression can be observed in animals grown at permissive
411 temperature (20 °C) (**Figure 3A**)^{10,28}. Exposure to heat stress (35 °C) induces expression of *hsp-*
412 *70*, as indicated by RFP expression of the reporter in the pharynx, spermatheca, intestine and
413 bodywall muscle (**Figure 3A**). This can be quantified, by measuring RFP fluorescence intensity
414 using Image J software (**Figure 3B**), as described in step 3.3 of the protocol section.
415

416 Constitutive knockdown of *hsp-90* in the intestine by *hsp-90* hairpin RNAi activates TCS¹⁰ and
417 results in a 20-fold upregulation of the *hsp-70p::RFP* reporter in primarily the bodywall muscle
418 cells (but not detectably in other tissues) at permissive temperature (**Figure 3A,3B**).
419

420 To identify components that trigger the TCS-mediated induction of *hsp-70* expression from the
421 intestine to the muscle, we performed a tissue-specific candidate RNAi screen of 58 candidate
422 genes (see **Figure 4A** for an experimental flow chart). The candidate genes were identified in a
423 preceding forward genetic screen and transcriptome analysis as potential modifiers of TCS in the
424 *hsp-90^{int} hp-RNAi* strain (**Figure 4**); and consisted of components involved in cellular signaling
425 processes, such as kinases, transcription factors and membrane proteins. We next wanted to
426 determine in which tissue the candidate genes were acting as enhancers or suppressors of TCS-
427 induced *hsp-70* expression in the muscle. This is achieved by measuring reduced (enhancer) or
428 increased (suppressor) *hsp-70p::RFP* fluorescence intensity of the reporter.
429

430 To perform the tissue-specific RNAi screen we first genetically crossed the *hsp-90^{int} hp-RNAi*
431 strain into *C. elegans* expressing SID-1 in either intestine or muscle. Intestinal SID-1 expression
432 allows to screen for potential TCS signaling components acting in the intestine to mediate TCS,
433 which is the tissue that perceives stress as reduced levels of *hsp-90*. Likewise, muscle specific SID-
434 1 expression allows for screening TCS components required in the responding muscle tissue. The
435 58 candidate genes used for the tissue-specific RNAi screen were termed *txt* (*tcs-(x)cross-tissue*).
436 Animals were grown on RNAi plates for two generations until Day 1 of adulthood and *hsp-*
437 *70p::RFP* fluorescence intensity in the muscle was measured by ImageJ software. As shown in
438 **Figure 4**, RNAi-mediated knockdown of 58 candidate *txt* genes in the intestine (**Figure 4B**) or the
439 muscle (**Figure 4C**) resulted in a range of modifiers that either suppress or enhance *hsp-70*

440 induction in the muscle. RNAi of candidates that result in a significant increase of *hsp-70p::RFP*
441 fluorescence intensity indicate that the gene acts as a cell nonautonomous suppressor of TCS,
442 whereas a reduction of RFP fluorescence intensity indicates that the candidate gene functions as
443 an enhancer. The scored hits (enhancers/suppressors) can then be confirmed by measuring their
444 effect on endogenous *hsp-70* mRNA levels by qRT-PCR and using proteostasis sensors.

445

446 **Use of proteostasis sensors to monitor tissue-specific PN capacity.**

447 TCS-mediated induction of *hsp-70* expression protects against protein misfolding and
448 aggregation in a cell nonautonomous manner^{5,10}. Proteostasis sensors can be used to survey the
449 folding capacity in different tissues during stress conditions. These include endogenous,
450 metastable proteins such as for example a conditional (temperature-sensitive; *ts*) mutant of
451 myosin expressed exclusively in the bodywall muscle (*unc-54(ts)*)²⁹ or proteins containing
452 expanded stretches of glutamine (PolyQ)^{30–32} (See **Table 3** for a list of strains). Proteins within a
453 length of 35-40 glutamines are particularly useful for this purpose, as they aggregate in an age-
454 and stress-dependent manner and are thus highly suitable to report on the folding environment
455 in specific tissues. These include strains expressing Q40::YFP in the neurons or Q35::YFP in the
456 muscle and Q44::YFP in the intestine^{30–32}. In addition to using PolyQ aggregation as a read-out,
457 strains expressing Q40::YFP or Q35::YFP also exhibit an age-dependent motility defect³⁰, allowing
458 quantification of motility by measuring thrashing rates in an automated manner (see ³³ for a
459 detailed example).

460

461 Here, we co-expressed intestinal Q44::YFP³² in strains allowing for tissue-specific RNAi via SID-1
462 complementation. RNAi-mediated knockdown of *hsp-90* at L4 stage in the neurons, intestine or
463 bodywall muscle, which induces TCS¹⁰, resulted in a reduced accumulation of intestinal Q44
464 aggregates in Day 2 adults compared to control animals (**Figure 5**). Thus, this indicates that the
465 TCS-mediated cell nonautonomous upregulation of *hsp-70* expression protects against age-
466 associated protein misfolding in multiple tissues of *C. elegans*.

467

468 **FIGURE AND TABLE LEGENDS:**

469 **Figure 1. Hairpin RNAi for constitutive gene knockdown in specific tissues.** (A) The inverted
470 repeats of *hsp-90* are generated by head-head ligation through a *SfiI* site (blue) introduced at one
471 end of each repeat. The inverted repeats are under control of a tissue-specific promoter for either
472 muscle- (*unc-54p*), neuron- (*rgef-1p*) or intestine- (*vha-6p*) specific expression. (B) The tissue-
473 specific expression of the inverted *hsp-90* repeats will produce hairpin-loop RNA that induces
474 tissue-specific RNAi in a strain with a *sid-1(pk3321)* mutant genetic background.

475

476 **Figure 2. Tissue-specific expression of SID-1 to enhance tissue-selective RNAi-mediated**
477 **knockdown.** (A) Overexpression of HSP-90::RFP in the neurons of RNAi-resistant *sid-1(pk3321)*
478 mutants. Expression of SID-1 in the neurons (*unc-119p::SID-1*) (strain PVH16); in the intestine
479 (*vha-6p::SID-1*) (strain PVH17); and muscle (*myo-3p::SID-1*) (strain PVH18) enhances RNAi
480 sensitivity in these specific tissues. Animals were exposed to *hsp-90* RNAi bacteria after L4 stage
481 for 24 hours, leading to visibly reduced neuronal-specific HSP-90::RFP fluorescence intensity in
482 the *unc-119p::SID-1* expressing animals only. Neurons in the tail region of the nematodes are
483 magnified. (B) Overexpression of HSP-90::RFP in the intestine of RNAi-resistant *sid-1(pk3321)*

484 mutants. Expression of SID-1 in the neurons (*unc-119p::SID-1*) (strain PVH19); in the intestine
485 (*vha-6p::SID-1*) (strain PVH20); and muscle (*myo-3p::SID-1*) (strain PVH21) enhances RNAi
486 sensitivity in these specific tissues. Animals were exposed to *hsp-90* RNAi bacteria after L4 stage
487 for 24 hours, leading to visibly reduced intestine-specific HSP-90::RFP fluorescence intensity in
488 the intestine of *vha-6p::SID-1* expressing animals only. (C) Overexpression of HSP-90::RFP in the
489 bodywall muscle of RNAi-resistant *sid-1(pk3321)* mutants. Expression of SID-1 in the neurons
490 (*unc-119p::SID-1*) (strain PVH22); in the intestine (*vha-6p::SID-1*) (strain PVH23); and muscle
491 (*myo-3p::SID-1*) (strain PVH24) enhances RNAi sensitivity in these specific tissues. This is
492 indicated by a visibly reduced HSP-90::RFP fluorescence intensity in the muscle of *myo-3p::SID-1*
493 expressing animals, but not in *unc-119p::SID-1* or *vha-6p::SID-1* expressing animals or control
494 animals (*sid-1(pk3321)*) that are resistant to RNAi in all tissues. Yellow arrows indicate the red
495 fluorescent pharyngeal co-injection marker (*myo-2p::RFP*). Scale bar = 50 μ m.

496

497 **Figure 3. Expression of intestine-specific *hsp-90* hairpin RNAi induces the heat-inducible *hsp-***
498 ***70p::RFP* reporter at permissive temperature in the muscle. (A)** Flow chart demonstrating the
499 tissue-specific RNAi screening protocol using stress reporters and tissue-specific proteostasis
500 sensors. (B) Fluorescent microscope images of animals expressing the *hsp-70* promoter fused to
501 red fluorescent protein (RFP) and in the background of *sid-1(pk3321)* mutants (control) (strain
502 AM994). Animals were either grown at 20°C (no HS) or treated with 1-hour heat shock at 35°C
503 (HS) and allowed to recover for 6 hours post-HS. *hsp-90^{intestine} hp-RNAi* animals (strain PVH2)
504 express an *hsp-90* hairpin RNAi construct under control of the intestine-specific promoter (*vha-*
505 *6p*) in the genetic background of *hsp-70p::RFP;sid-1(pk3321)*. Scale bar = 100 μ m (C)
506 Quantification of RFP fluorescence intensity of control animals grown at 20°C (no HS), treated
507 with a 1h HS at 35°C (HS) or expressing intestine-specific *hsp-90* hairpin RNAi at permissive
508 temperature (20°C). Bar graphs represent the average of 3 biological replicates; error bars
509 represent S.E.M. P-values were calculated using student's t test. *P < 0.05.

510

511 **Figure 4. Tissue-specific RNAi screen to identify modifiers of transcellular chaperone signalling.**
512 (A) Intestine-specific RNAi screen by feeding dsRNA bacteria to *hsp-90^{intestine} hp-RNAi* animals
513 expressing *vha-6p::SID-1* (strain PVH172; see Table 1 for genotype). Shown are candidate genes
514 that act as potential modifiers of TCS (**txt for intestinal tcs-(x)cross-tissue**) by either suppressing
515 or enhancing the *hsp-70p::RFP* fluorescence intensity in the bodywall muscle when knocked
516 down in the intestine. (B) Muscle-specific RNAi screen by treating *hsp-90^{intestine} hp-RNAi* animals
517 expressing *myo-3p::SID-1* (strain PVH171; see **Table 1**) with *txt* candidate gene RNAi. (A and B)
518 Fluorescence intensity of candidate genes are indicated as gray bars and are normalized to
519 control (EV) RNAi which is indicated as a black bar. Error bars are S.E.M. of 5 biological replicates.
520 The statistical significance of decreased or increased RFP fluorescence intensity between *txt* gene
521 RNAi compared to empty vector (EV) control RNAi was calculated using student's t test, and
522 correction for multiple testing was performed using the Benjamini-Hochberg method with a false
523 discovery rate of 0.05. * P < 0.05.

524

525 **Figure 5. Tissue-specific *hsp-90* RNAi reduces intestinal Q44::YFP (iQ44) aggregation. (A & B)**
526 Expression of intestinal Q44::YFP in the background of RNAi-resistant *sid-1(pk3321)* mutant allele

527 (strain PVH228) leads to accumulation of Q44 foci by Day 2 of adulthood. RNAi-mediated
528 knockdown by feeding *E. coli* expressing *hsp-90* dsRNA from L4 stage onwards is ineffective
529 compared to control RNAi (EV). (C & D) Neuron-specific (strain PVH229), (E & F) intestine-specific
530 (strain PVH230) or (G & H) muscle-specific *hsp-90* RNAi (strain 231) leads to reduced
531 accumulation of iQ44 foci at Day 2 of adulthood. (B, D, F, H) Quantification of the number of Q44
532 foci in worms exhibiting age-dependent Q44 aggregation at Day 1 and Day 2 of adulthood. Error
533 bars are S.E.M of 3 biological replicates. Statistical significance between *hsp-90* and empty vector
534 (EV) RNAi at Day 1 or Day 2 of adulthood was calculated using a student's t test. *n.s.* not
535 significant; *P < 0.05; **P < 0.01.

536

537 **Table 1. List of strains used in this work.**

538

539 **Table 2. Worm Lysis Buffer.**

540

541 **Table 3. List of proteostasis sensor- and stress reporter strains.**

542

543 **DISCUSSION:**

544 The methods described here demonstrate the use of tools that allow for the tissue-specific
545 knockdown of PN components in a constitutive and temporal manner. We have previously
546 identified TCS, a cell nonautonomous stress response mechanism that is induced by tissue-
547 specific alteration of Hsp90 expression levels¹⁰. Tissue-specific knockdown of *hsp-90* by
548 expression of hairpin RNAi leads to cell nonautonomous upregulation of protective *hsp-70*
549 chaperone expression in distal tissues, that increases organismal stress resistance¹⁰. We however
550 do not know which signaling components in the stress-perceiving or responding tissue are
551 activated to initiate this protective response. To identify signaling components mediating this
552 process, tissue-specific reverse genetic screens are one of the important methods of choice.

553

554 Although tissue-specific knockdown by expression of a hairpin construct can be effective, this has
555 disadvantages when a larger number of genes needs to be surveyed. Using RNAi-resistant *sid-1*
556 mutants complemented by expression of SID-1 in intestine, neurons or muscle allows for tissue-
557 specific gene knockdown by feeding RNAi and is thus an amenable tool for tissue-specific genetic
558 screens. While we here described a small-scale RNAi screen of 58 candidate genes, the tissue-
559 specific SID-1 system can be adapted for larger scale or genome-wide RNAi screens. For this, *C.*
560 *elegans* growth in a 96-well plate format and automated scoring of fluorescence intensity by a
561 plate reader will be required.

562

563 While the *sid-1* system can be effective for tissue-specific RNAi, an alternative method takes
564 advantage of *rde-1*, an Argonaute protein that functions cell-nonautonomously to mediate
565 systemic RNAi capacity¹³. Tissue-specific promoters driving *rde-1* rescue constructs also allow for
566 RNAi to be effective in specific tissues, similar to the *sid-1* system³⁴. However, *rde-1* mutations
567 used in the *rde-1* system rely on a RDE-1 E411K missense mutation that may not completely
568 abrogate RDE-1 function and so could lead to leakiness of RNAi activity in other tissues^{34,35}. This
569 issue however seems to be eliminated by the use of a newly generated *rde-1(mkc36)* indel
570 mutation³⁵. A particular current advantage of the *rde-1* system compared to the *sid-1* system is

571 the recent adaptation of the *rde-1* system for specific and effective RNAi in the germline³⁵. This
572 is important, as other currently existing germline-specific RNAi strains can also exhibit RNAi
573 efficiency in the soma. Thus, the *rde-1* system allowing for germline RNAi could be a useful tool
574 for researchers investigating the importance of the germline in various biological processes, such
575 as for example aging research.

576
577 This method is based on multicopy expression of integrated tissue-specific SID-1 arrays. To
578 achieve more physiological expression levels of SID-1 in the specific tissues, a CRISPR-Cas9
579 mediated single-copy knock-in method at defined genomic loci could be adapted for future use
580 of the *sid-1* system and to express SID-1 under control of tissue-specific promoters³⁶.

581
582 To investigate stress pathway activation, one has the choice of a large selection of transcriptional
583 chaperone reporters fused to green or red fluorescent proteins (**Table 3**). Tissue-specific
584 (intracellular) stress as opposed to environmental stress, may also lead to a differential tissue
585 expression profile of chaperone reporters, as shown by the results in **Figure 3**. For example, while
586 heat stress leads to induction of the *hsp-70p::RFP* reporter in multiple tissues (muscle,
587 spermatheca, pharynx, intestine), *hsp-90* hairpin RNAi in the intestine results in strong
588 upregulation of *hsp-70* in the muscle (**Figure 3A**). This may indicate that muscle cells are more
589 sensitive to changes in cell nonautonomous *hsp-90* levels, however it cannot be excluded that
590 *hsp-70* is also induced in other tissues, albeit not visibly with the transcriptional reporter fused
591 to a red fluorescent protein.

592
593 Therefore, proteostasis sensors are an important alternative, as they report on the actual folding
594 environment or capacity of the PN in a specific tissue. The folding environment is not only
595 dependent on chaperone expression, but also on PN components that regulate clearance of
596 misfolded protein such as autophagy or UPS. For example, if enhanced folding capacity is
597 indicated by one of the well-established folding sensors, but this does not overlap with increased
598 chaperone expression, then this may suggest that other components of the PN are activated that
599 increase proteostasis in a specific tissue. For example *hsp-4* is primarily induced in the intestine
600 when the cell nonautonomous UPR is activated in the neurons, yet the accumulation of misfolded
601 proteins expressed in muscle cells is also suppressed, possibly via lysosome activating signals
602 from the intestine³. Likewise, the data shows that *hsp-90* RNAi in the intestine delays iQ44
603 aggregation in the intestine (**Figure 5**), even though expression of the *hsp-70* reporter was not
604 detected in the same tissue (**Figure 3**). Thus in addition to folding sensors that report on the
605 folding environment in a given tissue, reporters for autophagic flux such as *Cherry::GFP::LGG-1*³⁷
606 or reporters that indicate the activity of the UPS such as *UbG76V::Dendra2*³⁸ expressed in
607 different tissues are just as crucial.

608
609 Taken together, we have described a tissue-specific RNAi system that allows for the examination
610 of the PN capacity in different tissues in response to a cell nonautonomously activated stress
611 response mechanism.

612
613 **ACKNOWLEDGMENTS:**

614 We thank Dr. Richard I. Morimoto for providing strain AM722. Some *C. elegans* strains used in
615 this research were provided by the Caenorhabditis Genetics Center, which is funded by the NIH
616 Office of Research Infrastructure Programs (P40 OD010440).
617 P.v.O.-H. was funded by grants from the NC3Rs (NC/P001203/1) and by a Wellcome Trust Seed
618 Award (200698/Z/16/Z). J.M. was supported by a MRC DiMeN doctoral training partnership
619 (MR/N013840/1).

620

621 **DISCLOSURES:**

622 The authors have nothing to disclose.

623

624 **REFERENCES:**

- 625 1. Morimoto, R. I. The heat shock response: systems biology of proteotoxic stress in aging
626 and disease. *Cold Spring Harbor Symposia on Quantitative Biology*. **76**, 91–99 (2011).
- 627 2. Hipp, M. S., Kasturi, P., Hartl, F. U. The proteostasis network and its decline in ageing.
628 *Nature Reviews Molecular Cell Biology*. **20**, 421–435 (2019).
- 629 3. Imanikia, S., Özbey, N. P., Krueger, C., Casanueva, M. O., Taylor, R. C. Neuronal XBP-1
630 Activates Intestinal Lysosomes to Improve Proteostasis in *C. elegans*. *Current Biology* **29**, 2322-
631 2338.e7 (2019).
- 632 4. Berendzen, K. M. et al. Neuroendocrine Coordination of Mitochondrial Stress Signaling
633 and Proteostasis. *Cell*. **166**, 1553-1563.e10 (2016).
- 634 5. O’Brien, D. et al. A PQM-1-Mediated Response Triggers Transcellular Chaperone
635 Signaling and Regulates Organismal Proteostasis. *Cell Reports*. **23**, 3905–3919 (2018).
- 636 6. Tatum, M. C. et al. Neuronal Serotonin Release Triggers the Heat Shock Response in
637 *C. elegans* in the Absence of Temperature Increase. *Current Biology*. **25**, 163–174 (2015).
- 638 7. Miles, J., Scherz-Shouval, R., van Oosten-Hawle, P. Expanding the Organismal
639 Proteostasis Network: Linking Systemic Stress Signaling with the Innate Immune Response.
640 *Trends in Biochemical Sciences*. **44**, 927–942 (2019).
- 641 8. Taylor, R. C., Dillin, A. XBP-1 Is a Cell-Nonautonomous Regulator of Stress Resistance and
642 Longevity. *Cell*. **153**, 1435–1447 (2013).
- 643 9. Prahlad, V., Cornelius, T., Morimoto, R. I. Regulation of the Cellular Heat Shock Response
644 in *Caenorhabditis elegans* by Thermosensory Neurons. *Science*. **320**, 811–814 (2008).
- 645 10. van Oosten-Hawle, P., Porter, R. S., Morimoto, R. I. Regulation of Organismal
646 Proteostasis by Transcellular Chaperone Signaling. *Cell*. **153**, 1366–1378 (2013).
- 647 11. Frakes, A. E. et al. Four glial cells regulate ER stress resistance and longevity via
648 neuropeptide signaling in *C. elegans*. *Science*. **367**, 436–440 (2020).
- 649 12. Timmons, L., Fire, A. Specific interference by ingested dsRNA. *Nature*. **395**, 854 (1998).
- 650 13. Tabara, H., Grishok, A., Mello, C. C. RNAi in *C. elegans*: soaking in the genome sequence.
651 *Science*. **282**, 430–431 (1998).
- 652 14. Hinas, A., Wright, A. J., Hunter, C. P. SID-5 is an endosome-associated protein required
653 for efficient systemic RNAi in *C. elegans*. *Current Biology*. **22**, 1938–1943 (2012).
- 654 15. Winston, W. M., Molodowitch, C., Hunter, C. P. Systemic RNAi in *C. elegans* Requires the
655 Putative Transmembrane Protein SID-1. *Science*. **295**, 2456–2459 (2002).
- 656 16. McEwan, D. L., Weisman, A. S., Hunter, C. P. Uptake of extracellular double-stranded
657 RNA by SID-2. *Molecular Cell*. **47**, 746–754 (2012).

- 658 17. Whangbo, J. S., Weisman, A. S., Chae, J., Hunter, C. P. SID-1 Domains Important for
659 dsRNA Import in *Caenorhabditis elegans*. *G3 GenesGenomesGenetics*. **7**, 3887–3899 (2017).
- 660 18. Feinberg, E. H., Hunter, C. P. Transport of dsRNA into cells by the transmembrane
661 protein SID-1. *Science*. **301**, 1545–1547 (2003).
- 662 19. Calixto, A., Chelur, D., Topalidou, I., Chen, X., Chalfie, M. Enhanced neuronal RNAi in *C.*
663 *elegans* using SID-1. *Nature Methods*. **7**, 554–559 (2010).
- 664 20. Kamath, R. S. et al. Systematic functional analysis of the *Caenorhabditis elegans* genome
665 using RNAi. *Nature*. **421**, 231–237 (2003).
- 666 21. Lee, Y. S., Carthew, R. W. Making a better RNAi vector for *Drosophila*: use of intron
667 spacers. *Methods (San Diego CA)*. **30**, 322–329 (2003).
- 668 22. Evans, T. Transformation and microinjection. *WormBook*.
669 doi:10.1895/wormbook.1.108.1 (2006)
- 670 23. Fay, D. Genetic mapping and manipulation: Chapter 1-Introduction and basics.
671 *WormBook*. doi:10.1895/wormbook.1.90.1 (2006)
- 672 24. Lim, M. A. et al. Reduced Activity of AMP-Activated Protein Kinase Protects against
673 Genetic Models of Motor Neuron Disease. *Journal of Neuroscience*. **32**, 1123–1141 (2012).
- 674 25. Stiernagle, T. Maintenance of *C. elegans*. *WormBook*. doi:10.1895/wormbook.1.101.1
675 (2006)
- 676 26. Hawkins, M. G., McGhee, J. D. elt-2, a second GATA factor from the nematode
677 *Caenorhabditis elegans*. *Journal of Biological Chemistry*. **270**, 14666–14671 (1995).
- 678 27. Bharadwaj, S., Ali, A., Ovsenek, N. Multiple components of the HSP90 chaperone
679 complex function in regulation of heat shock factor 1 In vivo. *Molecular and Cellular Biology*. **19**,
680 8033–8041 (1999).
- 681 28. Guisbert, E., Czyz, D. M., Richter, K., McMullen, P. D., Morimoto, R. I. Identification of a
682 tissue-selective heat shock response regulatory network. *PLoS Genetics*. **9**, e1003466 (2013).
- 683 29. Ben-Zvi, A., Miller, E. A., Morimoto, R. I. Collapse of proteostasis represents an early
684 molecular event in *Caenorhabditis elegans* aging. *Proceedings of the National Academy of
685 Sciences of the United States of America*. **106**, 14914–14919 (2009).
- 686 30. Morley, J. F., Brignull, H. R., Weyers, J. J., Morimoto, R. I. The threshold for
687 polyglutamine-expansion protein aggregation and cellular toxicity is dynamic and influenced by
688 aging in *Caenorhabditis elegans*. *Proceedings of the National Academy of Sciences of the United
689 States of America*. **99**, 10417–10422 (2002).
- 690 31. Brignull, H. R., Moore, F. E., Tang, S. J., Morimoto, R. I. Polyglutamine Proteins at the
691 Pathogenic Threshold Display Neuron-Specific Aggregation in a Pan-Neuronal *Caenorhabditis
692 elegans* Model. *Journal of Neuroscience*. **26**, 7597–7606 (2006).
- 693 32. Mohri-Shiomi, A., Garsin, D. A. Insulin Signaling and the Heat Shock Response Modulate
694 Protein Homeostasis in the *Caenorhabditis elegans* Intestine during Infection. *Journal of
695 Biological Chemistry*. **283**, 194–201 (2008).
- 696 33. Nussbaum-Krammer, C. I., Neto, M. F., Brielmann, R. M., Pedersen, J. S., Morimoto, R. I.
697 Investigating the spreading and toxicity of prion-like proteins using the metazoan model
698 organism *C. elegans*. *Journal of Visualized Experiments*. 52321 (2015)
- 699 34. Qadota, H. et al. Establishment of a tissue-specific RNAi system in *C. elegans*. *Gene*. **400**,
700 166–173 (2007).

- 701 35. Zou, L. et al. Construction of a germline-specific RNAi tool in *C. elegans*. *Scientific*
702 *Reports*. **9**, 1–10 (2019).
- 703 36. Silva-García, C. G. et al. Single-Copy Knock-In Loci for Defined Gene Expression in
704 *Caenorhabditis elegans*. *G3 Bethesda Md.* **9**, 2195–2198 (2019).
- 705 37. Chang, J. T., Kumsta, C., Hellman, A. B., Adams, L. M., Hansen, M. Spatiotemporal
706 regulation of autophagy during *Caenorhabditis elegans* aging. *eLife*. **6**, e18459 (2017).
- 707 38. Hamer, G., Matilainen, O., Holmberg, C. I. A photoconvertible reporter of the ubiquitin-
708 proteasome system in vivo. *Nature Methods*. **7**, 473–478 (2010).
- 709

Figure 1

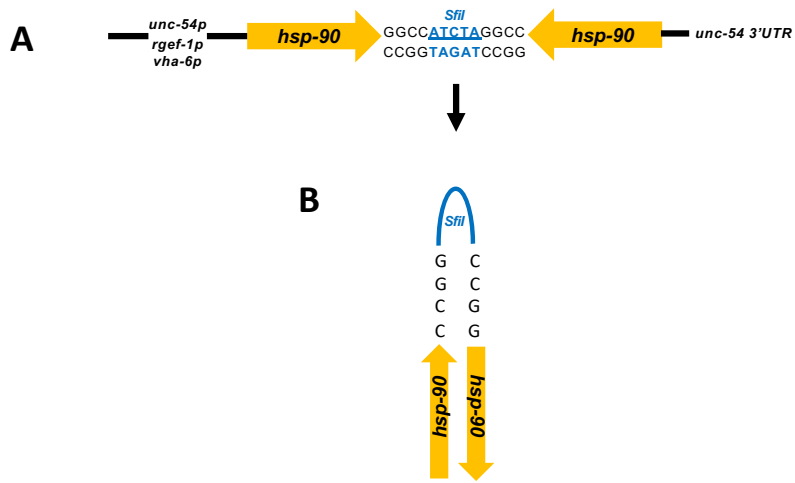


Figure 2

Tissue-specific RNAi by SID-1 complementation

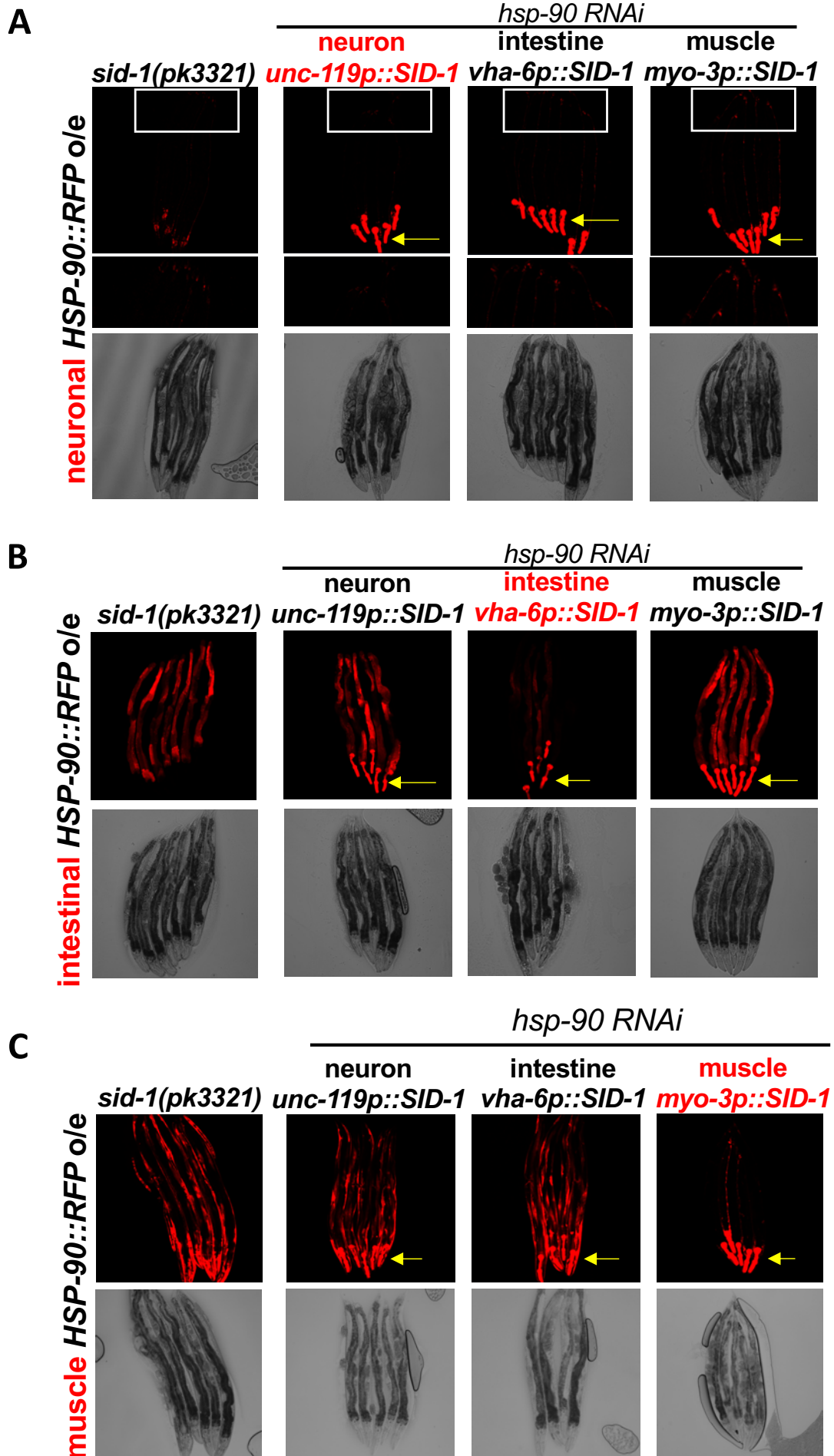
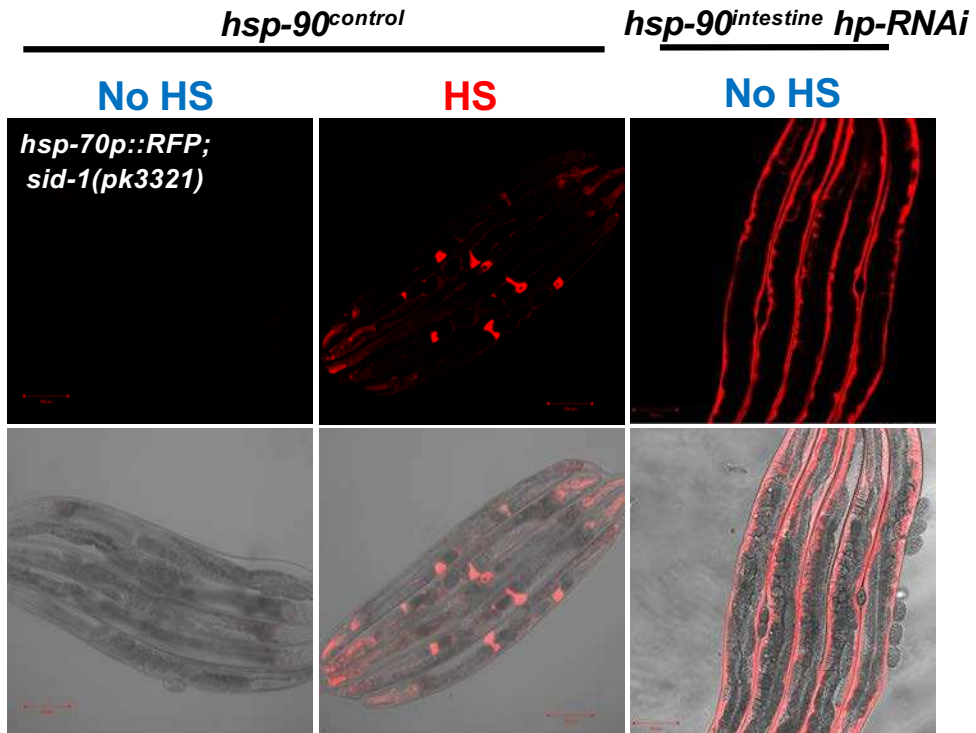


Figure 3

A



B

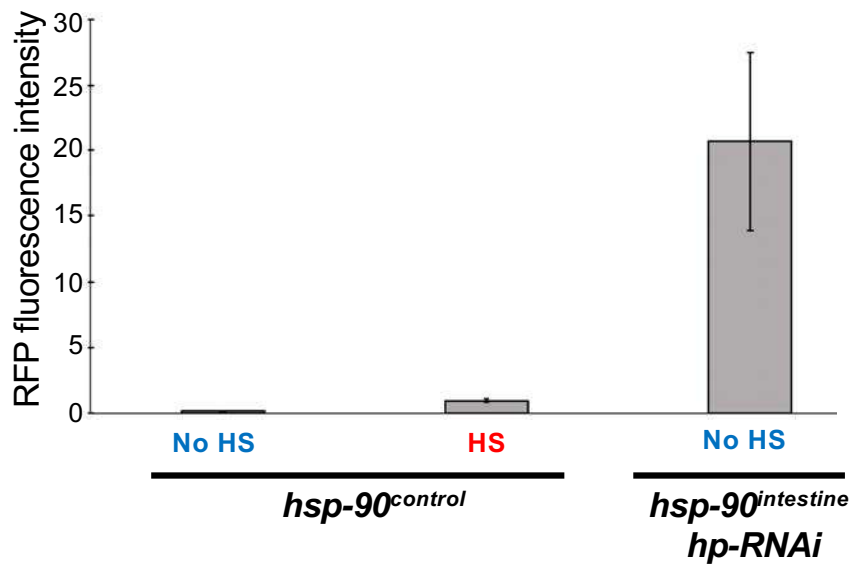
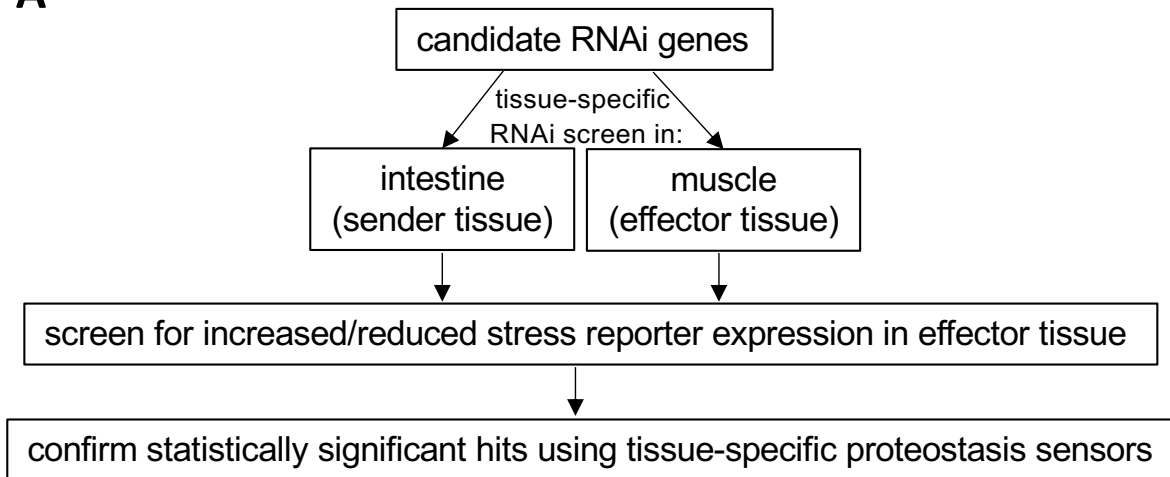
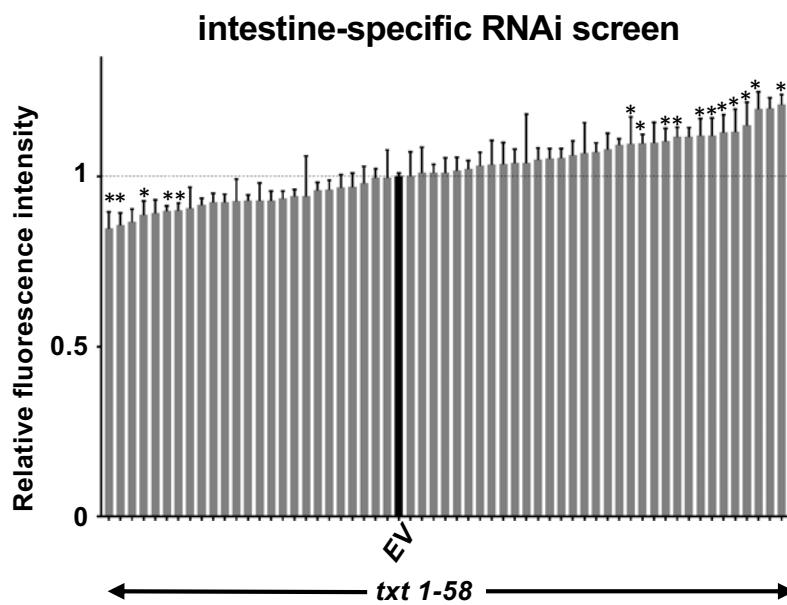


Figure 4

A



B



C

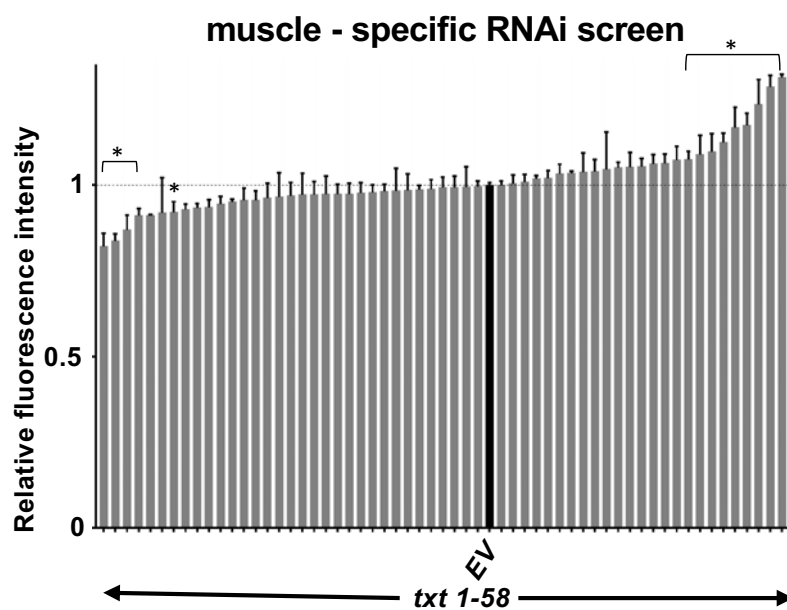


Figure 5

